

A modelling study using WRF-Chem over north India with improved transport and waste burning emissions

Saurabh Annadate
MS16016

*A dissertation submitted for the partial fulfilment
of BS-MS dual degree in Science*

Under the guidance of
Dr. Vinayak Sinha



April 2021

Indian Institute of Science Education and Research Mohali
Sector - 81, SAS Nagar, Mohali 140306, Punjab, India

Certificate of Examination

This is to certify that the dissertation titled "**A modelling study using WRF-Chem over north India with improved transport and waste burning emissions**" submitted by Mr. Saurabh Annadate (Reg. No. MS16016) for the partial fulfilment of the BS-MS dual degree programme of the Institute, has been examined by the thesis committee duly appointed by the Institute. The committee finds the work done by the candidate satisfactory and recommends that the report be accepted.



Dr. Raju Attada



Dr. Anoop Ambili



Dr. Vinayak Sinha

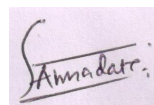
(Supervisor)

Dated: 28.04.2021

Declaration

The work presented in this dissertation has been carried out by me under the guidance of Dr. Vinayak Sinha at the Indian Institute of Science Education and Research Mohali.

This work has not been submitted in part or in full for a degree, a diploma, or a fellowship to any other university or institute. Whenever contributions of others are involved, every effort is made to indicate this clearly, with due acknowledgment of collaborative research and discussions. This thesis is a bonafide record of original work done by me and all sources listed within have been detailed in the bibliography.



Saurabh Annadate
(Candidate)

Dated: April 28, 2021

In my capacity as the supervisor of the candidate's project work, I certify that the above statements by the candidate are true to the best of my knowledge.



Dr. Vinayak Sinha
(Supervisor)

Acknowledgement

First and foremost, I would like to thank my thesis supervisor Dr. Vinayak Sinha, without whose help and supervision, this thesis would have never been possible. The discussions that I had with him has enhanced my capabilities as a researcher. I am thankful for his guidance and time for this project, even during the pandemic. I would like to thank Dr. Baebel Sinha for her valuable inputs on this project. I would like to thank Dr. Abhishek Mishra for teaching me the WRF-Chem model and helping me throughout the project. I would also like to thank Dr. J. Gowrishankar, Director, IISER Mohali, for providing a conducive environment which was very helpful for completing the thesis in time.

I would like to take this opportunity to express my gratitude to my parents for all their hard work and support. I want to thank my caring sister and lovely nephew for constantly motivating me. I also acknowledge my labmates for their help.

I acknowledge the Atmospheric Chemistry Observations and Modeling Lab (ACOM) of NCAR for providing the WRF-Chem pre-processor tools. I acknowledge the Atmosphere Monitoring Service (CAMS) and Copernicus Climate Change Service (C3S) data for providing ERA5 reanalysis data.

Saurabh Annadate

MS16016

IISER Mohali.

List of Figures

1.1	shows the PMF resolved factors related to the road transport sector at IISER Mohali. It displays the normalized source fingerprints of the PMF factors and samples collected at the source in bar-chart form. Normalized species contribution is denoted by red squares on the right axis. The high emissions of BTEX species from the road-transport sector reported.[5] (under Creative Commons Attribution 4.0 License: https://www.atmospheric-chemistry-and-physics.net/policies/licence_and_copyright.html)	3
2.1	The data flow diagram of the WRF model	8
2.2	2.2a represents the topographic height(in meters) of the terrain made using the pre-processors. 2.2b represents the vegetation classified into different MODIS land-use categories. The map shows the distribution of these categories over the modelling domain.	9
2.3	The algorithm followed by MEGAN to calculate BVOC emission.	11
2.4	Yellow box marks the modelling domain of this study. Precise location of IISER-Mohali Atmospheric chemistry facility (30.667° N, 76.729°E) is represented by the yellow dot in the center.	13
2.5	shows the meteorological parameters simulated by the default model. 2.5a shows the time series of the temperature extracted over Mohali compared with the measured temperature at the IISER atmospheric facility. 2.5b shows the variation in the planetary boundary layer height compared with the ERA5 data.	14
2.6	Newly computed PFT maps taken from Mishra <i>et al.</i> , 2021. (a) Needle leaf tree fraction, (b)broad leaf tree fraction, (c)shrub fraction, and (d) herb fraction.[24]	16
2.7	represents new isoprene emission potential(mg of isoprene m ⁻² s ⁻¹) map over India. 17	

2.8	shows the leaf area index maps taken from the ERA5 reanalysis product. 2.8a is a map of LAI of the high vegetation class, and 2.8b represents LAI corresponding to the low vegetation class.[30]	18
2.9	show the vegetation fraction maps taken from ERA5 reanalysis product for the period of May 2012. 2.9a represents the high vegetation cover and 2.9b represents the low vegetation cover.[30]	18
2.10	The time series of (a)temperature and (b)PBLH simulated by the improved model compared with the published results of Mishra <i>et al.</i> , 2021. The traces of ground measurements and the default model are added for reference.	19
2.11	The gridded maps of waste burning emission of CO, NO _x , NH ₃ , BC, OC, SO ₂ from the OWBEII. The emissions are in the units of g/year[15].	24
3.1	The meteorological parameters simulated using the default model extracted over Mohali and compared with ground measurement data. 3.1a shows the time series of temperature, 3.1b shows the time series of PBLH compared with the ERA5 reanalysis product, and 3.1c is the solar radiation time series plot against the ground measurement data.	26
3.2	Time series of the criteria air pollutants like carbon monoxide(CO) and nitrogen oxides(NO _x) along with the NMVOCs toluene and acetone simulated by the default model. Modelled quantities are plotted along the left axis and ground measurement based quantities are plotted along the right axis.	27
3.3	The time series of (a) toluene, (b) NO _x , (c) acetaldehyde, and (d) CO for default and improved road-transport model extracted over Mohali.	29
3.4	The spatial maps of the average emissions of acetaldehyde, toluene, NO _x , acetone, and CO. The emissions of the default model(column 1),after using improved transport emissions(column 2), and the percentage difference between two scenarios(column 3){ $(\text{improved emission}-\text{default emission}) \times 100/\text{default emission}$ } at each grid point is shown. The total percentage difference is calculated using average of emissions over complete domain for entire simulation.	30
3.5	The time series of (a) acetaldehyde, (b) toluene, (c) CO, and (d) propene for default and improved road transport and waste burning model extracted over Mohali. Modelled quantities are plotted along the left axis and ground measurement based quantities are plotted along the right axis.	32

- 3.6 The gridded maps of the average emissions of acetaldehyde, toluene, NO_x , acetone, and CO. The emissions of the default model(column 1), the improved road transport and waste burning model(column 2), and the percentage difference between two scenarios(column 3) $\{(\text{improved emission}-\text{default emission})\times 100/\text{default emission}\}$ are shown. The total percentage difference is calculated using average of emissions over complete domain for entire simulation. 33
- 3.7 The time series of difference between the emissions of two modelling scenarios: with improved road transport and waste burning emissions minus with improved road transport emissions for (a) acetaldehyde and (b) toluene extracted over Mohali. 34

List of Tables

1.1	Comparison of estimates of India's anthropogenic emissions in 2000. Emissions are in kt year^{-1} . Estimates are excluding emissions from fossil fuel use for international aviation, international shipping, and open biomass burning[1].	2
1.2	Estimated emissions from open waste burning sector in India and increment relative to MIX-Asia inventory[16].	5
2.1	The processes of WRF-Chem and the corresponding parametrization used in the simulation.	21

Notation

EDGAR	Emission Database for Global Atmospheric Research
FINN	Fire INventory from NCAR
GOCART	Global Ozone Chemistry Aerosol Radiation and Transpor
MEGAN	Model of Emissions of Gases and Aerosols from Nature
MOZART	Model for Ozone and Related chemical Tracers
OWBEII	open waste burning emission inventory of India
PBLH	Planetary Boundary Layer Height
PFT	Plant Functional Type
RTEII	Road transport emission inventory for India
WRF-Chem	Weather Reasearch Forecast model coupled with Chemistry

Contents

Acknowledgement	i
List of Figures	v
List of Tables	vii
Notation	ix
Abstract	xiii
1 Introduction	1
1.1 The road transport emission sector	1
1.2 The Waste burning emission sector	4
2 Materials and methods	7
2.1 Model description	7
2.2 Modelling Setup	7
2.2.1 WRF Pre-processing system (WPS)	8
2.2.2 ARW Solver	9
2.2.3 Emission Inventories	10
2.3 Model validation over the domain of interest	12
2.3.1 Default model setup	13
2.3.2 Improved model setup	15
2.3.3 Validation of the modelling setup	19
2.4 Addition of improved road-transport and waste burning inventories to the WRF-Chem setup	20
2.4.1 The WRF-Chem model setup	20

2.4.2	Modifying the EDGARv4.3.2 inventory	21
3	Results and discussions	25
3.1	Results of the default model simulation	25
3.2	Sensitivity of the new road-transport emission inventory(RTEII)	28
3.3	Results of adding the waste burning sector to EDGARv4.3.2	31
4	Summary and conclusion	35
A	Important codes for the input files used in WRF-Chem	37
A.1	Anthropogenic emission input file	37
A.2	Fire emission input file	38
	Bibliography	39

Abstract

Anthropogenic emissions can affect the local, regional, and global air quality and climate considerably. It has changed the earth's energy budget and increased global warming. The road transport sector is one of the major contributors to anthropogenic emissions of India. Road transport significantly degrades air quality by emitting volatile organic compounds and ozone precursors. It increases tropospheric ozone production and affects human health severely. The open waste burning sector is very poorly represented in the global emission inventories. It significantly pollutes regional air quality by emitting particulate matter and other air pollutants. In this work, we study road transport and open waste burning emissions using the WRF-Chem regional transport model. We set up the WRF-Chem model and validated it using the published results for the north Indian modelling domain. Then we applied it to study the air quality changes in the criteria air pollutants and volatile organic compounds over North India. We incorporated the improved road transport emission inventory and open waste burning emission inventory from India(OWBEII) into the WRF-Chem model. For the model simulation of 14 days(1May-14May, 2012), the use of improved road transport emission inventory relative to the EDGARv4.3.2 significantly increased modelled emissions of acetaldehyde(24%), toluene(23%), NO_x (23%), acetone(13%), and decreased CO(-8%). The use of improved road transport and OWBEII waste burning inventory in the model further increased the modelled emissions of acetaldehyde(35%), toluene(30%), NO_x (26%) and acetone(17%) relative to the EDGARv4.3.2.

Chapter 1

Introduction

The development of a reliable anthropogenic emission inventory is important for regional transport modelling. It is also vital for understanding the atmospheric chemistry of the region to take effective pollution control measures. Increasing population, technology, and connectivity are changing the world faster, hence needing updated emission inventories. In the last three decades, the energy consumption of Asia has doubled, causing rapid growth in emissions, by 28% for BC, 64% for CO, 108% for NMVOC, 119% for SO₂, and 176% for NO_x [1]. Quantifying emissions accurately over India is very challenging because of the technology mix, lack of accurate measurements, vast population segregated in different economic levels, etc. Recently various efforts were made to develop reliable emission inventories over Asia and India. According to the Regional Emission inventory in ASia (REAS) Version 1.1, India emitted 6140 kt SO₂, 4730 kt NO_x, 795 kt BC, 3268 kt OC, 79382 kt CO, and 8638 kt NMVOC in the year 2000[1]. But many inventories give different estimates based on different approaches used while calculating emissions. The Table 1.1 summarizes the total anthropogenic emission estimates of India for the year 2000 given by different inventories. We will particularly look at the road transport and waste burning emissions over India.

1.1 The road transport emission sector

The road transport emission sector is one of the major contributors to the anthropogenic emission budget of India. It significantly impacts stratospheric ozone depletion and climate change. Road traffic emissions have been the cause of concern about air quality and its

Inventory projects	REASv1.1	TRACE-P	EDGARv3.2	IIASA
SO ₂	6140	5462	7846	5919
NO _x	4730	4047	6285	4563
BC	795	517	–	–
OC	3268	2190	–	–
CO	79382	51081	58631	96753

Table 1.1: Comparison of estimates of India’s anthropogenic emissions in 2000. Emissions are in kt year^{−1}. Estimates are excluding emissions from fossil fuel use for international aviation, international shipping, and open biomass burning[1].

effect on human health and tropospheric ozone production[2]. Additionally, the transport sector is a significant contributor to global carbon dioxide (CO₂) emissions. Worldwide 20% of total fossil fuel were used by the road transport sector and contributed 23% of total energy-related CO₂ emissions in 2012[3]. The total number of registered vehicles in the country has increased from 55 to 173 million from 2001 to 2013, with an annual growth rate of 9.2% in the vehicle population[4]. A study by Singh et al. estimates the emissions from the road transport sector in India using the vehicle kilometre travelled approach revealed a compound annual growth rate of around 9% for CO₂, CH₄, NO_x, CO, SO₂, PM, and HC emissions from 2001 to 2013[3].

A quantitative source apportionment study using the US EPA PMF 5.0 Model for volatile organic compounds measured at the IISER Mohali facility showed 24.8% contribution from cars and two-wheeler to the total VOC emission budget. The Figure 1.1 shows the significant emissions of BTEX (benzene, toluene, ethylbenzene, and xylene) compounds associated with traffic emissions using the PMF model. That shows the importance of the road transport sector over the Mohali site.

This rapid growth in the transport sector calls for the updated emission inventory. The EDGARv4.3.2 reports the total NMVOCs emission from the road transport sector in India to be 2.1 kilotons[6]. But the emission factors and the activity data used for this study is out of date now. So we have used the latest Road Transport Emission Inventory of India(RTEII) for this study which reports toluene, isopentane , and acetaldehyde to be the top three VOCs from the transport sector. This study shows that the EDGARv4.3.2 significantly

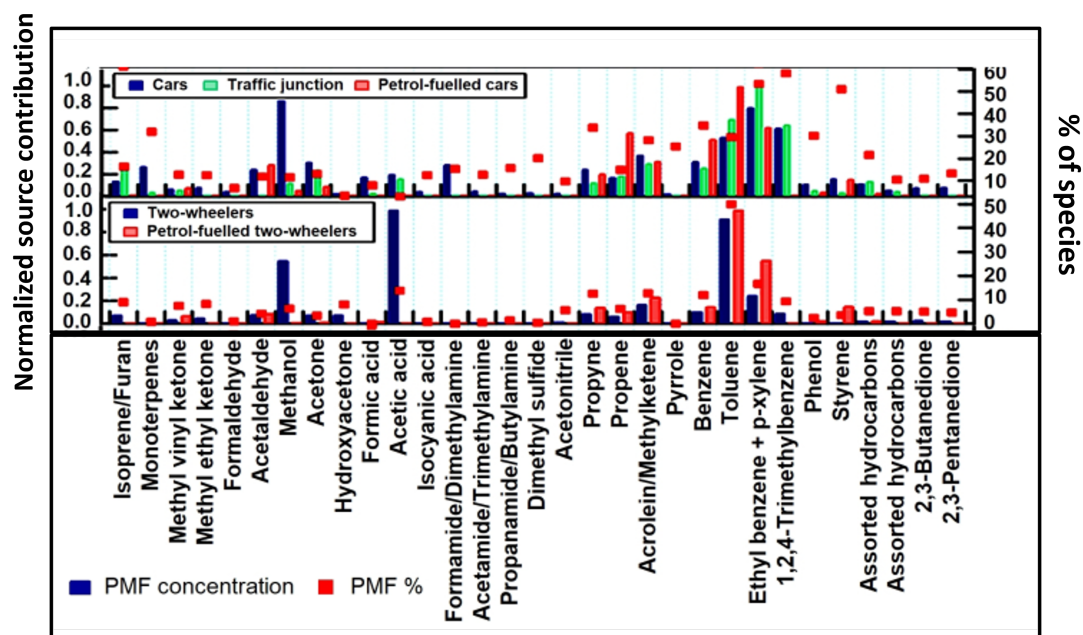


Figure 1.1: shows the PMF resolved factors related to the road transport sector at IISER Mohali. It displays the normalized source fingerprints of the PMF factors and samples collected at the source in bar-chart form. Normalized species contribution is denoted by red squares on the right axis. The high emissions of BTEX species from the road-transport sector reported.[5] (under Creative Commons Attribution 4.0 License: https://www.atmospheric-chemistry-and-physics.net/policies/licence_and_copyright.html)

overestimate the emissions of ethene, propene, ethylbenzene, 2,2- dimethyl butane, CO, NO_x while significantly underestimating acetaldehyde in India[7].

1.2 The Waste burning emission sector

The open waste burning emission is one of the most poorly represented sectors in the global emission inventories. Open waste burning happens at the individual household level as well as at the community level at the dumpsites by the municipalities. It is a large source of air pollution that degrades the air quality and affects human health adversely. It is reported that 1.2 kg of municipal solid waste(MSW) is generated per person per day, and by 2025 a total of 2200 Tg y⁻¹ MSW will get generated all over the world[8]. It will not be feasible to treat all the waste in a controlled environment since the developing countries still lack the required infrastructure to a great extent. To take suitable measures, we need to understand the emissions coming out of open waste burning. Global CO₂ emission from open waste burning is small compared to the total anthropogenic emission budget of CO₂, but at the regional level, particularly in developing countries like India, are substantial[9].

In India, bigger waste management challenges arise because of high population, poor waste segregation at source[10], unreliable waste collection, poor connectivity at remote places, etc. Many households burn MSW in the open[11], and even the municipal workers burn the waste in the open in some cases(sometimes despite having functional infrastructure)[12]. The officially acknowledged annual waste estimate of India is 49 Tg y⁻¹, which is concentrated only in urban India[13]. The Open Waste Burning Inventory from India(OWBEII)[14] reports the waste production for the year 2015 to be 216 Tg y⁻¹, from which 68 Tg y⁻¹ was burned in the open[15]. A significant increase of 8-12% was reported in India's NMVOC emission because of open waste burning. Table 1.2 represents the estimated emissions of criteria air pollutants and NMVOCs in India(OWBEII) and compared them with the MIX-Asia emission inventory.

Open waste burning contributes highly to the PM_{2.5} and PM₁₀ levels. 99.5% of the Indian population lives in regions that do not meet WHO air quality standards for fine particulate pollution[17]. Particulate matter has far more concerning health effects. Children and older people are more susceptible to lung diseases by inhaling PM_{2.5}. So it makes it important to study the emissions coming out of waste burning sector in order to make right mitigation

Pollutant	Increase in emission(Gg y⁻¹)	% increase relative to the MIX-Asia
NMVOC	1400-2000	8-12
BC	40-110	8-12
CO ₂	58000-130000	2-6
CO	3000-7000	4-11
Acetaldehyde	20-320	—
propene	50-170	—
ethene	50-190	—
benzene	30-280	—

Table 1.2: Estimated emissions from open waste burning sector in India and increment relative to MIX-Asia inventory[16].

policies.

Chapter 2

Materials and methods

2.1 Model description

In this project, we have used Weather Research and Forecasting model coupled with chemistry (WRF-Chem). This model simulates the emission, transport, mixing, and chemical transportation of trace gases and aerosols. This model is widely used to investigate regional-scale air quality, transport of chemical species, and interaction. WRF-Chem simulates meteorological fields online that reduce time-averaging errors. Online models do not require high-resolution meteorological datasets, thus give the upper hand over offline models. The WRF-Chem takes 2-way feedback in-between chemistry and meteorology. Therefore, it improves meteorological inputs and output forecast.

2.2 Modelling Setup

The Weather Research and Forecasting (WRF) model is well known for atmospheric research. The effort to develop WRF began in the latter 1990s with the collaborative work of NCAR, NOAA, the U.S Air Force, the Naval Research Laboratory, the University of Oklahoma, and the FAA. WRF has different components to address various tasks to be a complete model. The Figure2.1 shows the data flow and the three major constituents of WRF which are as follows:

- The WRF Preprocessing System (WPS)
- ARW solver

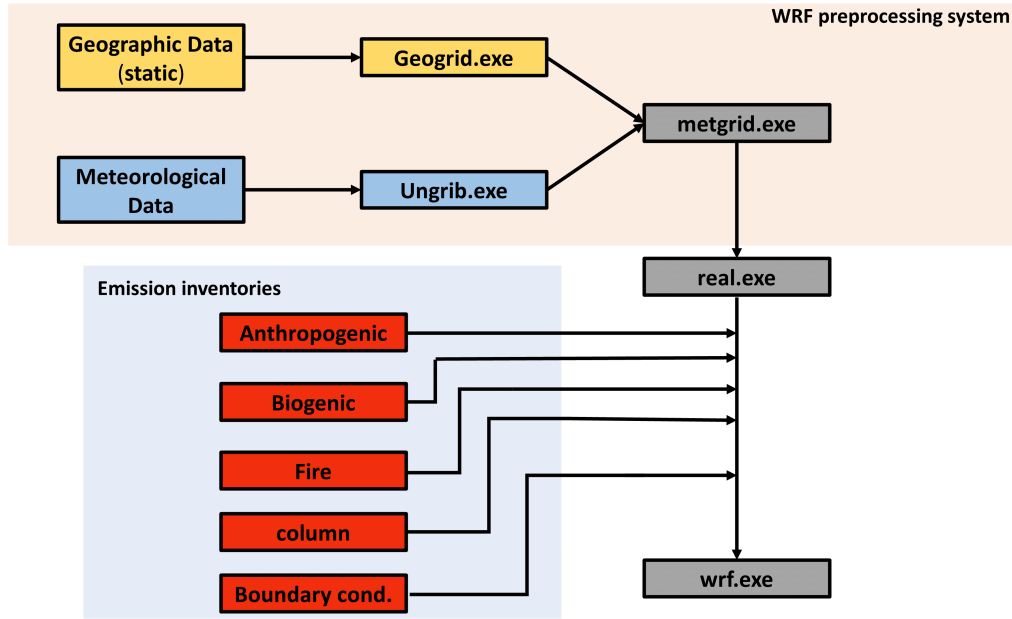


Figure 2.1: The data flow diagram of the WRF model

- Post-processing and Visualization tools

2.2.1 WRF Pre-processing system (WPS)

The WPS program is mainly used for real-data forecasting. Its primary function is to define the modelling domain and interpolate terrestrial data to the simulation domain. It also interpolates the meteorological data from the other model (global models in most cases) to our modelling domain. The WPS is composed of three applications which are as follows:

1. **Geogrid:** The area over which we want to do the scientific study is essential to define the mathematical model correctly. Geogrid defines the model domain using static geographic data. The simulation domain is constructed by the user using the input file called namelist.wps. This program computes latitude and longitude at every grid point. In addition, it interpolates soil categories, land use category, terrain height, annual mean deep soil temperature, monthly vegetation fraction, monthly albedo, maximum snow albedo, and slope category to the model grids.
2. **Ungrib:** This program is essential for extracting meteorological data in GRIB format to the intermediate format for further mapping on the modelling domain. Our simulation uses the NCEP Final analysis (FNL) data from (GFS) global forecasting system at 1° spatial resolution and 6 hourly temporal resolution[18].

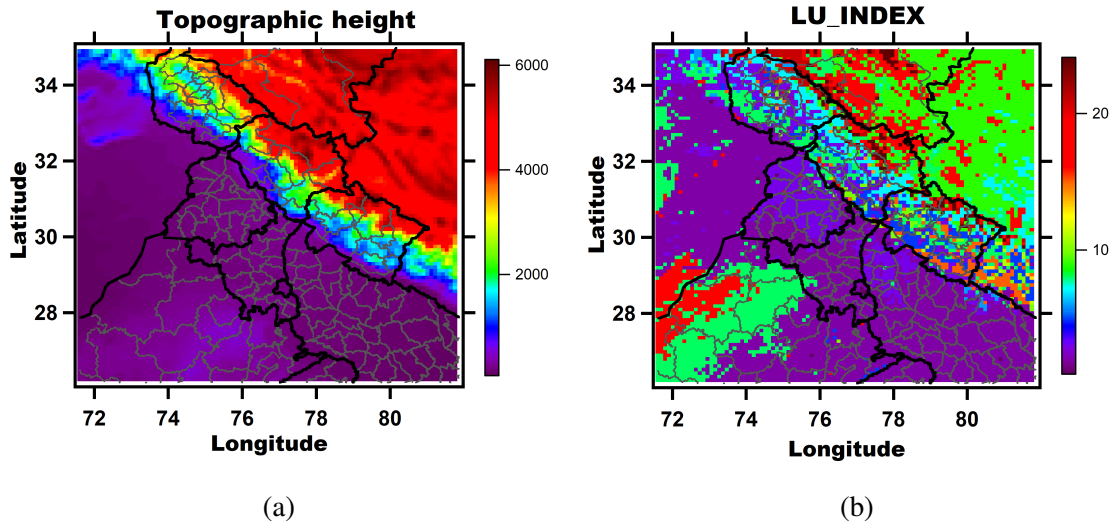


Figure 2.2: 2.2a represents the topographic height(in meters) of the terrain made using the pre-processors. 2.2b represents the vegetation classified into different MODIS land-use categories. The map shows the distribution of these categories over the modelling domain.

3. **Metgrid:** Metgrid uses the meteorological fields extracted using the ungrib program to interpolate onto the modelling domain defined by the geogrid program. Files made using this program are further fed into the WRF run. Output files of the metgrid will have geographical and meteorological fields' information over the simulation domain. The Figure2.2 represents the simulated geographical fields over our domain of interest.

2.2.2 ARW Solver

After preparing files that define the domain of interest, some required fields in the model need to be initialized. The WRF model has two classes of simulations, first is the 'ideal' case, and the second is the 'real' case. The ideal case is just a simplified mathematical model with ideal atmospheric and static fields which are not taken from any real dataset. WRF takes the meteorological and geographical data from the real data mapped by the preprocessing program in the 'real' case. The program named 'real.exe' is used to ingest the pre-processor's output files and make them ready for the WRF. The output file will have the name 'wrfinput.d01'. The output file will be a NetCDF file that should be visualized and checked before further processing. Anthropogenic, biogenic, and biomass burning emissions shall be mapped from various sources onto this file as initial conditions. The

mapping of these emissions from different inventories along with boundary conditions is discussed in the subsequent sections. Finally, the WRF solver program, 'wrf.exe', is run to start the model.

2.2.3 Emission Inventories

Accurate emission inventories are vital to produce closer to reality results from a transport model. It helps in improving spatial variability and agreement with ground measurement data. In the WRF-Chem, we can map the following emissions to the wrfinput_d01 file: anthropogenic, biogenic, and fire emission. Then lateral boundary and initial conditions from global chemistry model output are mapped. In this section, various emission types are discussed in detail.

- (a) **Anthropogenic emission:** The emission database for global atmospheric research (EDGARv4.3.2)[6], A global anthropogenic emission inventory has given by the European Commission, is used in this study. This inventory provides the sector-specific spatial distribution of the flux ($\text{kg m}^{-2}\text{s}^{-1}$) for the GHGs and other air pollutants for 2012. It has emissions of the following air pollutants, Ozone precursor gases: Carbon Monoxide (CO), Nitrogen Oxides (NO_x), Non-Methane Volatile Organic Compounds (NMVOC) and Methane (CH_4), Acidifying gases: Ammonia (NH_3), and Sulfur Dioxide (SO_2), Primary particulates: Fine Particulate Matter (PM10, PM2.5, BC, OC).

EDGAR comes in the spatial resolution of 0.1-degree x 0.1-degree. It consists the emission from the following sectors: Power Industry, Oil refineries and Transformation industry, Combustion for manufacturing, Aviation climbing and descent, Aviation cruise, Aviation landing and takeoff, Aviation supersonic, Road transportation, Non-metallic minerals production, Chemical processes, Iron and steel production, Non-ferrous metals production, Food and Paper, Non-energy use of fuels, Solvents and products use, Manure management, Agricultural soils, Agricultural waste burning, Solid waste landfills, Wastewater handling, Solid waste incineration, and Fossil Fuel Fires

- (b) **Biogenic emissions:** In this study, the biogenic emissions are calculated using the Model of Emissions of Gases and Aerosols from Nature (MEGAN) v2.04[19]. Since

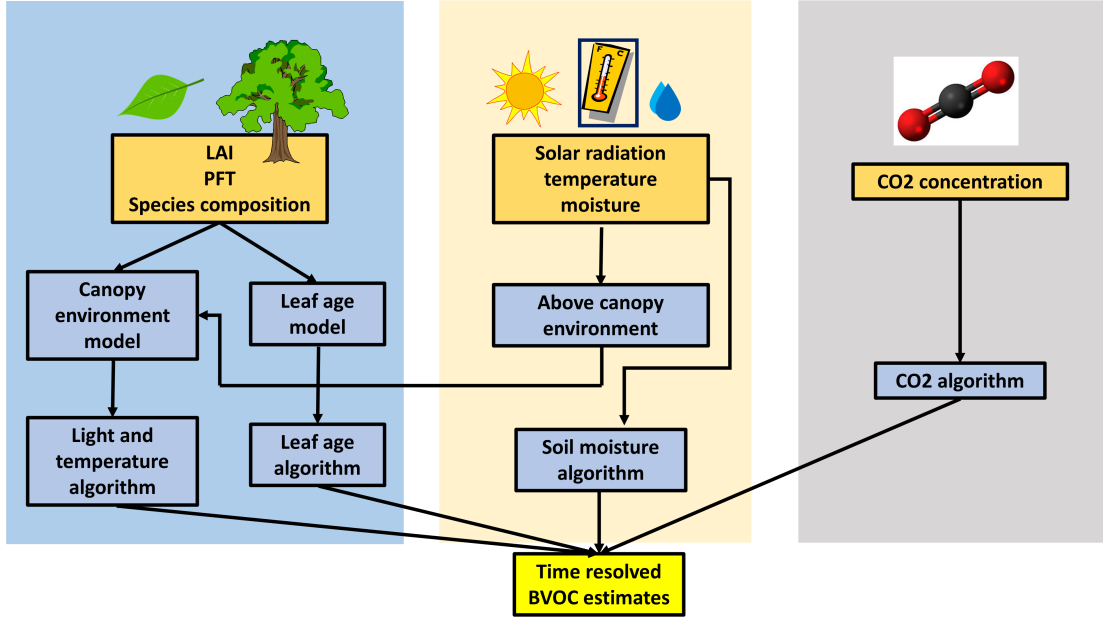


Figure 2.3: The algorithm followed by MEGAN to calculate BVOC emission.

this module is online, it calculates biogenic emissions at each timestep. It uses the gridded data of leaf area index (LAI), solar radiation, plant functional types, species composition of the area, etc. The Figure2.3 gives pictorial description of the MEGAN algorithm. Formula for the biogenic emission used in MEGAN is,

$$\text{emission} = [\epsilon][\gamma][\rho] \quad (2.1)$$

ϵ represents the emission factor at standard conditions, γ is an emission activity factor, and ρ is production and loss within the canopy. The previous version of MEGAN[20] assumed that all the emissions go entirely to the above atmosphere, but the latest version considers the loss from dry deposition and chemical loss within the canopy. The algorithm of the MEGAN model is represented by the fig above. It consists of different smaller modules that take care of different factors that affect BVOC emissions. It considers major processes that drive variations in emissions of VOC. Such as response to light, temperature, LAI, leaf age, soil moisture, and CO2 inhibition[21].

- (c) **Biomass burning emission:** The Indo-Gangetic plain, which is the focus of this study, is a very fertile land. It is widely covered with croplands and contributes significantly to the food basket of the South-Asian region. Because of large croplands, biomass burning is observed commonly in this region. Also, open biomass burning is

a significant contributor to the global emission budget of aerosols, VOCs, etc. Wheat residue burning increases daytime ozone levels[5]. Biomass burning mostly happens at night time because of the government regulations in India. That makes it difficult to detect. Different studies have shown that biomass burning is highly variable both temporally and spatially, showing a strong interannual and diurnal variability[22].

In this study, we have used Fire INventory from NCAR (FINN) dataset[23], which uses MODIS satellite to scan the fires worldwide. The fires are detected using channel 21 of the MODIS satellite. The fire detection algorithm takes into account the MODIS vegetation continuous field product, which has information about different vegetation classes.

2.3 Model validation over the domain of interest

To validate the WRF-Chem model setup over the North-India region, we decided to reproduce the already published results by Mishra *et al.*[24]. This study focuses on the impacts of vegetation on land-atmosphere interactions through isoprene emission, evapotranspiration, and photosynthesis. It is observed that biogenic emissions play a significant role in the atmospheric chemistry of the NW-IGP region. We aim to study the impact of BVOCs on meteorological parameters like temperature and boundary layer height using a similar experimental setup. This study focuses on the time period of August-2012. It was a monsoon season; rain clears out the emissions from other sources, giving us an excellent window to look at the biogenic emissions. In this study, We have run the model for two different scenarios, which are as follows:

1. **Default model:** In this case, we run the WRF-Chem model with the default configuration.
2. **Improved model:** In this case, we update the tree cover map in the MEGAN module, we update the LAI and vegetation fraction maps in the WRF input file.

Details about these two scenarios are discussed in the following sections. We then compare the results with the already published work. This exercise helped us gain confidence in our modelling setup. In addition, it helped to get acquainted with the WRF-Chem model.

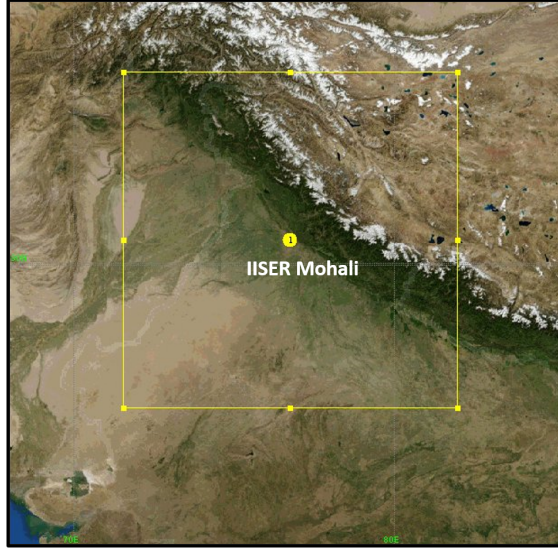


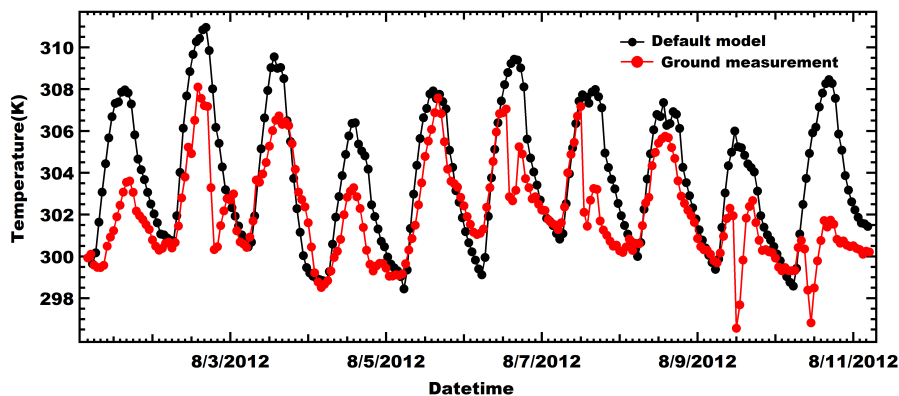
Figure 2.4: Yellow box marks the modelling domain of this study. Precise location of IISER-Mohali Atmospheric chemistry facility (30.667° N, 76.729° E) is represented by the yellow dot in the center.

2.3.1 Default model setup

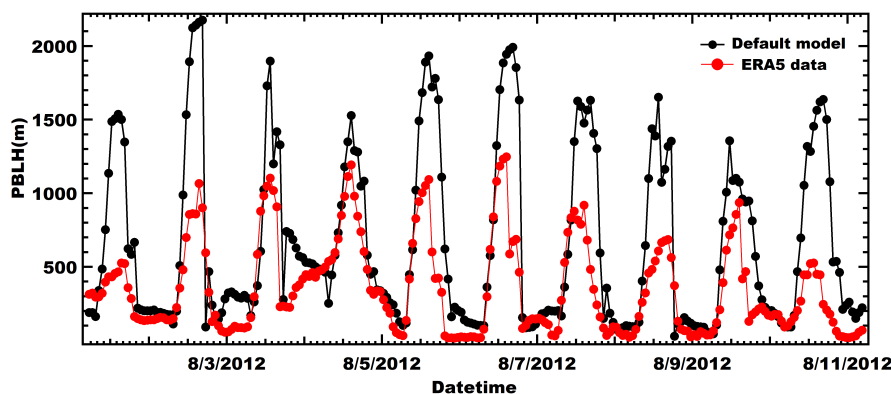
As shown in the Figure 2.4, a $1000 \times 1000 \text{ km}^2$ domain centred on 30.667° N, 76.729° E with horizontal resolution of 10 km is used in this simulation. The modelling domain is divided into 51 vertical levels from the surface to take into account the interactions between the troposphere and stratosphere in the high mountains of the Himalayas. We chose the first ten days of August 2012 during the monsoon season for this simulation.

The WRF-Chem is set up with the following schemes. Geographic static data as input to the geogrid program was taken from WRF mandatory static database. The meteorological initial and lateral boundary conditions were taken from the NCEP research data archive[18], which is available every 6 hours at a spatial resolution of $1^{\circ} \times 1^{\circ}$. Albedo, vegetation fraction, soil classification, terrain height, and similar fields were taken from the Modified IGBP MODIS land-use dataset[25]. The land surface processes are taken from the Noah land surface module[26]. Anthropogenic emissions are taken from the Emission Database for Global Atmospheric Research-Hemispheric Transport of Air Pollution (EDGAR-HTAP)[27]. Emissions of trace gas species from biomass burning are taken from the NCAR (FINN) v1 fire inventory[23]. Biogenic emissions of gases and aerosols are calculated online using MEGANv2.04[19]. Yonsei University planetary boundary layer scheme is used[28]. The MOZCART chemical scheme is used for model chemistry mech-

anisms. The chemical initial and lateral boundary conditions are provided by archived datasets of the MOZART-4 global 3-d chemical transport model[29]. Aerosols in the MOZ-CART mechanism are represented using the Global Ozone Chemistry Aerosol Radiation and Transport (GOCART) scheme.



(a)



(b)

Figure 2.5: shows the meteorological parameters simulated by the default model. 2.5a shows the time series of the temperature extracted over Mohali compared with the measured temperature at the IISER atmospheric facility. 2.5b shows the variation in the planetary boundary layer height compared with the ERA5 data.

The comparison plots in the Figure2.5 show that the default model setup is not able to produce an accurate representation of meteorological variables. The temperature recorded at the ground measurement facility is not in complete agreement with the default model. Specifically, the peak values of temperature have a discrepancy of 2-4 degrees on some days. On the other hand, lower values of temperature are in better agreement. Next, we have compared the planetary boundary layer height (PBLH) simulated by the model with

the ERA5 data extracted over Mohali. The planetary boundary layer is the air column extending up to the subsidence inversion. The vertical mixing of surface air is limited to this PBL height. PBLH is an important variable from the point of view of air pollution and transport. 2.5b shows that the default model has predicted much higher PBLH at the noontime. The night-time values are in agreement with the ERA5 data.

2.3.2 Improved model setup

As discussed earlier, modifications done to the default model were inspired by the study by Mishra *et al.* 2021. We changed the plant functional types maps(PFTs), leaf area index map(LAI), and vegetation fraction(vegfra) map in the model. These modifications are explained in further detail below.

- (A) **Plant functional types(PFTs):** In the MEGAN model, there are various emission factor schemes are discussed. Based on the functional type of a plant different emission factors are assigned to them. The number of plant functional types included in the scheme increases from PFT-1(1) to PFTREG(unlimited)[21]. The standard scheme that is used in our model is PFT-5 with the following PFTs: broadleaf trees, needle leaf trees, shrubs, herbs, and barren land. We have replaced the original PFT maps with the newly computed maps given by Mishra *et al.*, 2021 showed in Figure2.6. This map is created using the help of MODIS sensor derived Vegetation Continuous Field(VCF): MOD44B, and European Space Agency globe cover LULC dataset. The fractional tree cover for the South Asian modelling domain is created using both datasets. Globcover dataset is used to assign trees to each PFT depending upon the relevant LULC class[24].

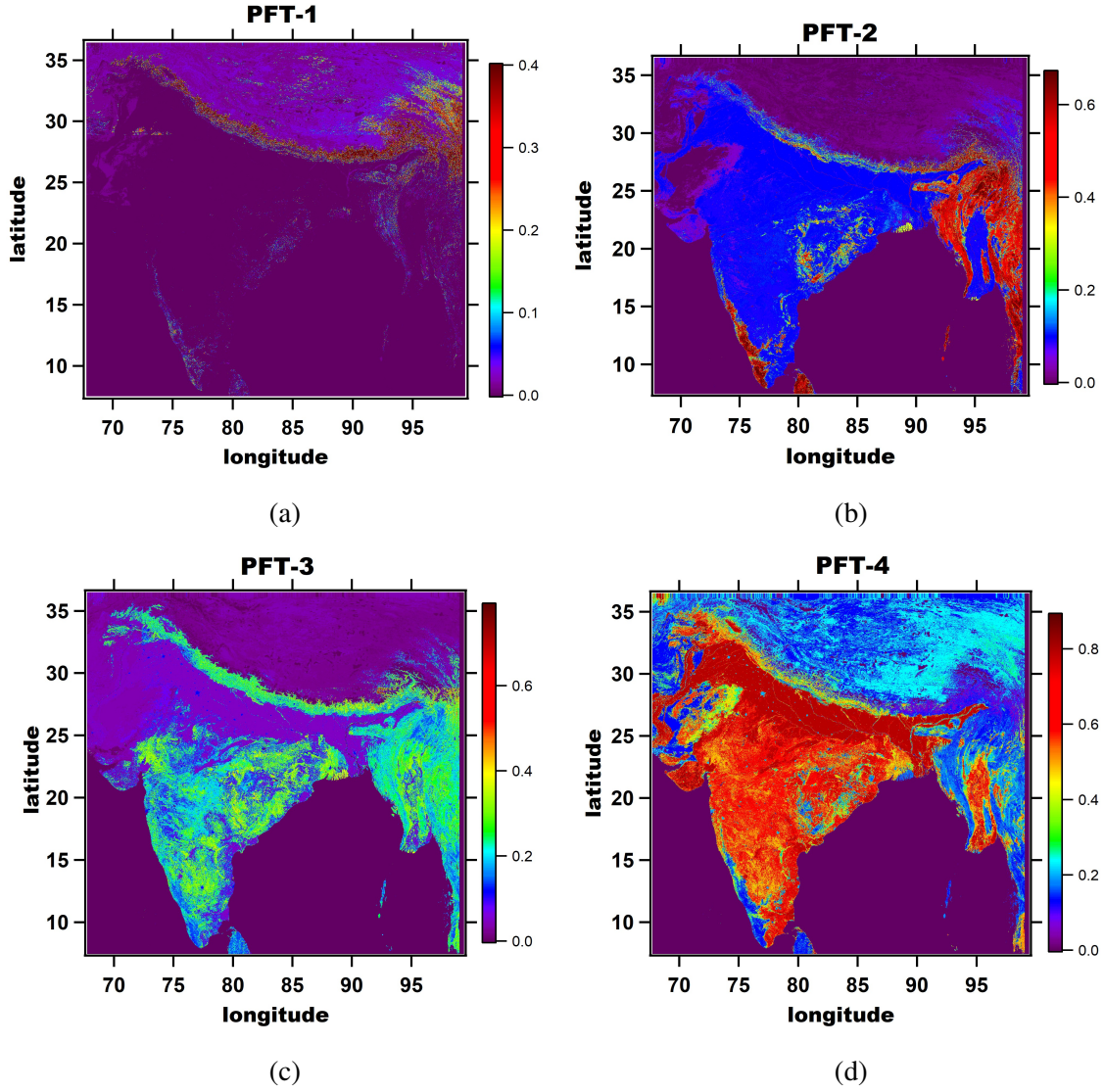


Figure 2.6: Newly computed PFT maps taken from Mishra *et al.*, 2021. (a) Needle leaf tree fraction, (b) broad leaf tree fraction, (c) shrub fraction, and (d) herb fraction.[24]

The values of global average isoprene emission factors are 12.6, 2.0, 10.7, and 0.5 ($\text{mg of isoprene m}^{-2}\text{s}^{-1}$) for broadleaf trees, needle leaf trees, shrubs, and herbs, respectively[19]. By multiplying the global emission factors and the PFT fraction and summing it over at each gridpoint, we calculated the isoprene emission potential at over India. The Figure2.7 shows the modified isoprene emission potential map.

(B) **Leaf area index(LAI)**: The WRF-chem is set to choose the land surface processes from the Noah land surface module. It is based on the Moderate Resolution Imaging Spectroradiometer - International Geosphere-Biosphere Programme (MODIS-IGBP) vegetation dataset. So we need to change the Noah model files for the new vegetation

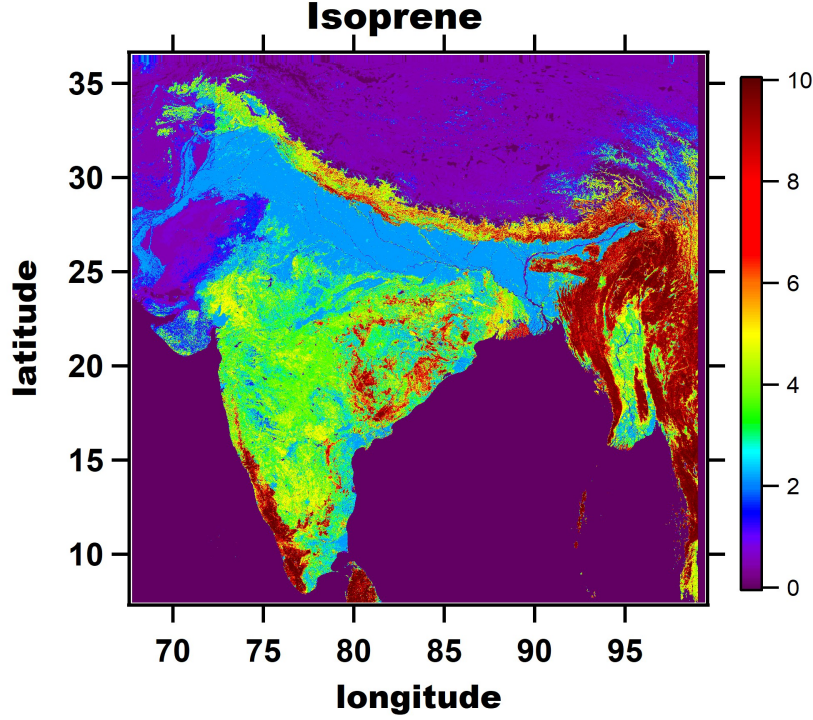


Figure 2.7: represents new isoprene emission potential(mg of isoprene $\text{m}^{-2}\text{s}^{-1}$) map over India.

data. It could have been more hectic to change the vegetation maps inside the code and run the initialization program. Therefore, we first created the initial WRF input file and then changed the variables like LAI and VEGFRA in the input file.

The new leaf area index map is taken from the ERA5 data[30] of August 2012, which is the period of our interest. This dataset has two types of vegetation classes. The high vegetation class includes broadleaf and needle leaf trees, whereas the low vegetation class consists of herbs, shrubs, and crops. The ERA5 data comes in a regular lat-lon grid of 0.25 degrees for the reanalysis and 0.5 degrees for the uncertainty estimate. As shown in the Figure 2.8, We took 0.25 degrees data and regridded it to 0.1 degrees to replace it in the WRF input file. Since the LAI for low and high vegetation is separate in the new dataset, we added both the quantities at all grid points. We used Python for extracting the exact area and replacing it in the input NetCDF file.

- (C) **Vegetation fraction(VEGFRA):** WRF has the variable named VEGFRA that represents the fraction of the pixel occupied by vegetation. Like LAI, we have taken vegetation fraction from ERA5 as well[30]. The procedure for modifying this variable also remains the same. First, we run the model with new PFT files and generate

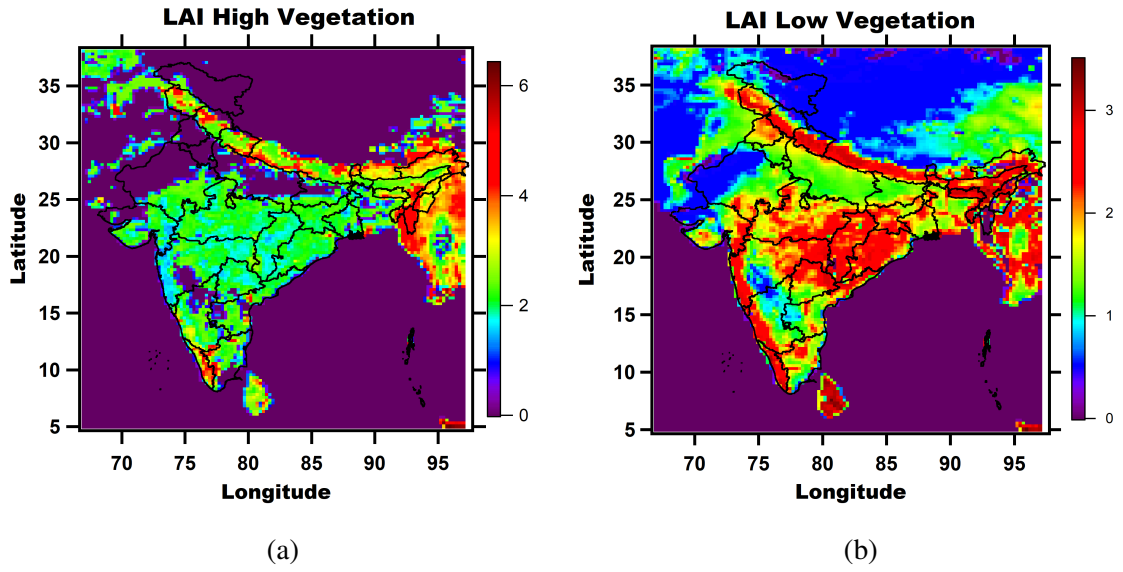


Figure 2.8: shows the leaf area index maps taken from the ERA5 reanalysis product. 2.8a is a map of LAI of the high vegetation class, and 2.8b represents LAI corresponding to the low vegetation class.[30]

the wrfinput file. Then we replace the corresponding variable in the wrfinput file with our gridded dataset using Python. Figure2.9 shows the ERA5 vegetation graphs for the month of May 2012 that are used in this simulation.

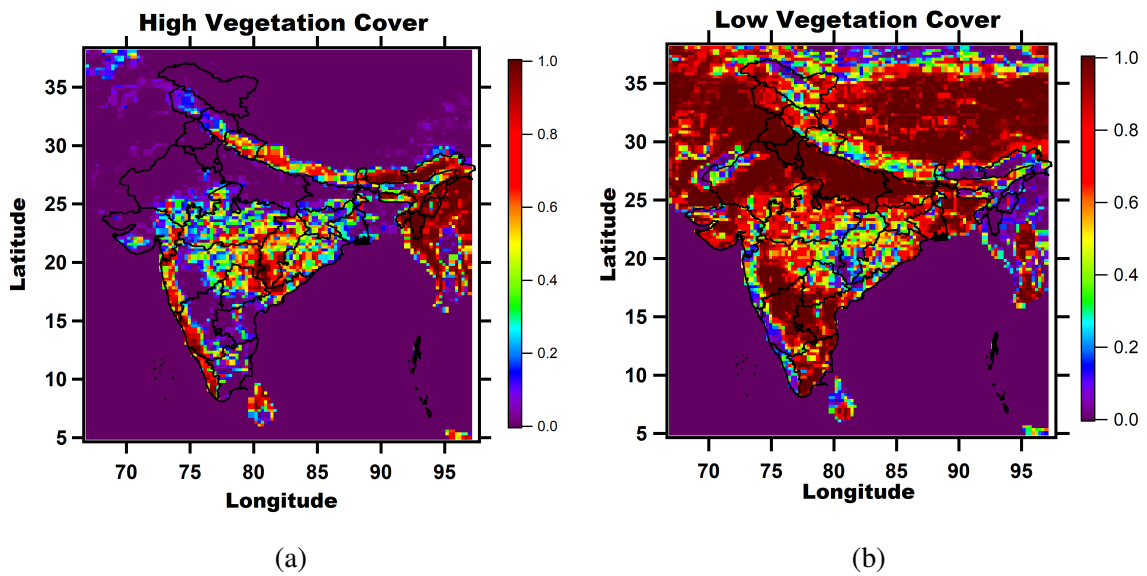
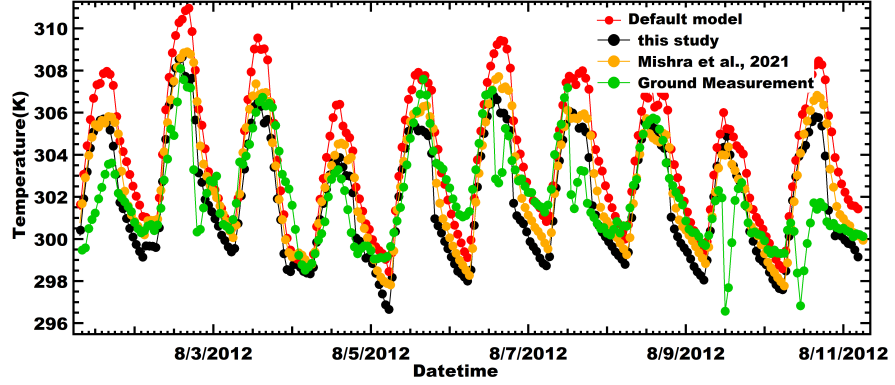


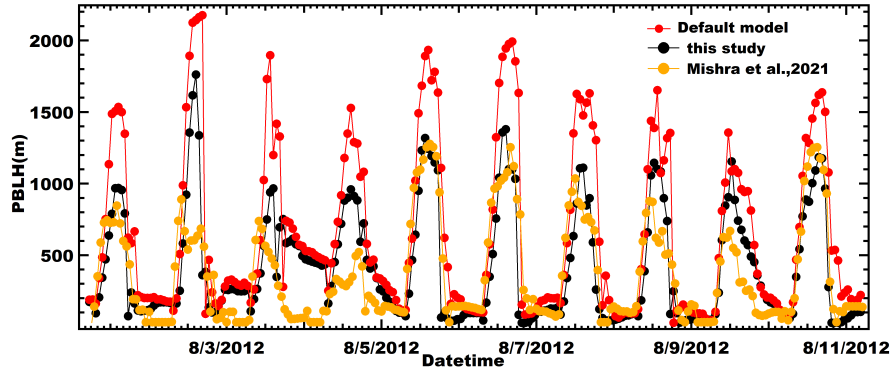
Figure 2.9: show the vegetation fraction maps taken from ERA5 reanalysis product for the period of May 2012. 2.9a represents the high vegetation cover and 2.9b represents the low vegetation cover.[30]

2.3.3 Validation of the modelling setup

We ran the model with the modifications mentioned above in the default setup. All parameters, other than the ones discussed above, were kept the same as the default simulation. The figure 2.10 compares the meteorological parameters of the improved model and the model results given by Mishra *et al.*, 2021. The traces of ground measurement and the default model are also appended for reference.



(a)



(b)

Figure 2.10: The time series of (a)temperature and (b)PBLH simulated by the improved model compared with the published results of Mishra *et al.*, 2021. The traces of ground measurements and the default model are added for reference.

Fig 2.10 clearly shows the mitigation in the peak temperature of the improved model from the default case. It agrees more with the model temperature data of Mishra *et al.*, 2021 and the ground measurement data. The PBLH also shows a similar trend. The peak boundary layer height has been reduced by around 500 meters on average. From 6 August 2012, PBLH matches more closely with the PBLH data simulated by Mishra *et al.*, 2021[24].

These results show the reproducibility of the published results with our model setup, which increases confidence in our modelling setup.

2.4 Addition of improved road-transport and waste burning inventories to the WRF-Chem setup

The emission inventories are vital to the atmospheric transport modelling setup. It is necessary to have accurate emissions to reproduce the spatial variability and agreement with ground data. In this study, we check the accuracy of EDGARv4.3.2 on the NW-IGP using the WRF-Chem transport model. We further study the sensitivity of the newly made Road-Transport Emission Inventory(RTEII) and Open Waste Burning Emission Inventory from India(OWBEII)[14][15] by incorporating them into the model.

For this study, we have set up three modelling scenarios to quantify changes in emissions from each new emission sector. In all the scenarios we have used EDGARv4.3.2 as a base emission inventory.

- (a) **Default model:** In this scenario, we run the model with default EDGARv4.3.2 emission inventory.
- (b) **Improved road-transport model:** In this scenario, we replace the road-transport sector of the EDGARv4.3.2 with the RTEII inventory.
- (c) **Improved transport and waste-burning model:** In this scenario, we replace the road-transport sector of the EDGARv4.3.2. In addition, we add the new waste burning sector.

2.4.1 The WRF-Chem model setup

In order to verify the accuracy of the EDGARv4.3.2 dataset, we have set up the WRF-Chem modelling domain over the North-India region, similar to the previous experiment. This time we chose the time period of May-2012 for the simulation. Because May is summertime, there is less perturbation to the planetary boundary layer height. In addition, biogenic emissions are also not that significant in this period, giving a good window to look at anthropogenic emissions.

Process/Parameter	Parametrization
Meteorological BCs	NCEP FNL (1°)
Surface Processes	Noah land surface model
PBL Parametrization	Yonsei boundary layer scheme
Biogenic Emission	MEGAN v4.02
Chemical Mechanism	MOZCART
Anthropogenic Emission	EDGAR v4.3.2
Biomass burning emission	NCAR-FINN
Chemical boundary conditions	MOZART-4
Chemical Mechanism	MOZCART
Resolved Scale Cloud Physics	Morrison 2-moment
Convective and Shallow Cloud	Grell-3D ensemble
Long and short wave radiation transfer	RRTM

Table 2.1: The processes of WRF-Chem and the corresponding parametrization used in the simulation.

The first few days of May-2012 were strongly affected by anthropogenic emissions. This was also the post-harvesting period in India, so the biomass burning events also lie in this period. We chose the time period of 1 to 14 May for this simulation with three days spinup time. We ran the model with 10km resolution over the North-India modelling domain. The feedback from the aerosol radiation was kept on in the simulation. The Table2.1 notes the parametrization used for each process in the model.

2.4.2 Modifying the EDGARv4.3.2 inventory

- (a) **Adding the improved road-transport sector:** The emission inventory of EDGARv4.3.2 relies on outdated emission factors of two decades or older vehicles. The rapid changes in technology in recent times change the emissions from vehicles significantly. In April 2010, emission standards for new vehicles were renewed to Bharat stage-3(which is equivalent to Euro-3) all over India. The continuous changes in population size, technology, and the transport sector make it necessary to update the emission inventories. For this study, we have used the newly created road-transport

emission inventory: RTEII(Road Transport Emission Inventory for India) [7]. The fuel consumption data for this inventory is taken from the national fuel consumption statistics report of the Ministry of Petroleum and Natural Gas, Government of India[31]. It also considers the fraction of fuel consumed by different types of vehicles and calculates the emissions. Since RTEII uses more recent activity data and emission factors, we expect it to produce better predictions with the transport model.

To replace the existing road-transport sector from the EDGAR netCDF files with new RTEII emissions, we needed to convert the road-transport inventory(RTEII) into a netCDF file format. The netCDF file format saves the data into a compact matrix format. The rows of the matrix represent latitudes, and the columns represent longitudes. Each element of the matrix takes the value corresponding to its lat-lon for a particular variable. The WRF-Chem model needs the total flux at each gridpoint, so we needed to change the units of RTEII. We divided each value(which was initially in kg/year) by the area of each grid cell and the total time of the year in seconds to convert it into the units of flux($\text{kg m}^{-2}\text{s}^{-1}$). EDGAR inventory comes with different files for each species. Each file consists of different variables for various emission sectors and a variable 'emis_sum' for holding the sum of all the sectors. The road-transport variable is named '1A3b' in the netCDF file. For updating the road-transport sector, we only replaced the emissions corresponding to the '1A3b'. We also updated the 'emis_sum' variable by adding emissions of all sectors.

- (b) **Adding the new waste burning sector:** Open waste burning and waste management are some of India's major problems, just like other developing countries. Municipal solid waste(MSW) includes plastic, paper, kitchen waste, biomedical waste, food waste, etc. The problem of segregating dry and wet waste is common and often leads to inefficient waste management. MSW is often burned in the open by citizens or even by the municipal authorities in the absence of proper infrastructure. Open waste burning is a significant contributor to many criteria air pollutants. It may also perturb atmospheric OH reactivity and ozone formation rates. Still, the waste burning sector is absent in the EDGAR to a large extent. The waste burning emissions are poorly represented in the global emission inventories, especially over India.

We have used the new open waste burning emission inventory for India(OWBEII)[15]

in this simulation to introduce the waste burning sector in the WRF-Chem model. OWBEII covers all the municipal solid waste for the sake of disposal. While computing the gridded emission database, OWBEII considers waste production disparity based on income, recycling rates, waste management practices in India, recovery of waste by municipalities, and emission factors calculated by the garbage fire experiments. It has a spatial resolution of $1^\circ \times 1^\circ$ that makes it easier to incorporate it into EDGARv4.3.2 for the simulation. Figure 2.11 represents the gridded emission maps of criteria pollutants from waste burning sector which have been used in this simulation.

The procedure to add the waste burning emissions to the already existing EDGAR files is very similar to replacing the road-transport sector.

- (a) Open the modified EDGARv4.3.2 file of any species in write mode. (We have used NetCDF library in Python to do this)
- (b) Introduce a new variable to hold gridded waste burning emission matrix
- (c) Fill this matrix with emissions from the corresponding species of OWBEII
- (d) Update the 'emis_sum' variable
- (e) Close the file and repeat the same procedure for all other species

Once we added the waste burning sector to all species files, we put them into its working directory in the code.

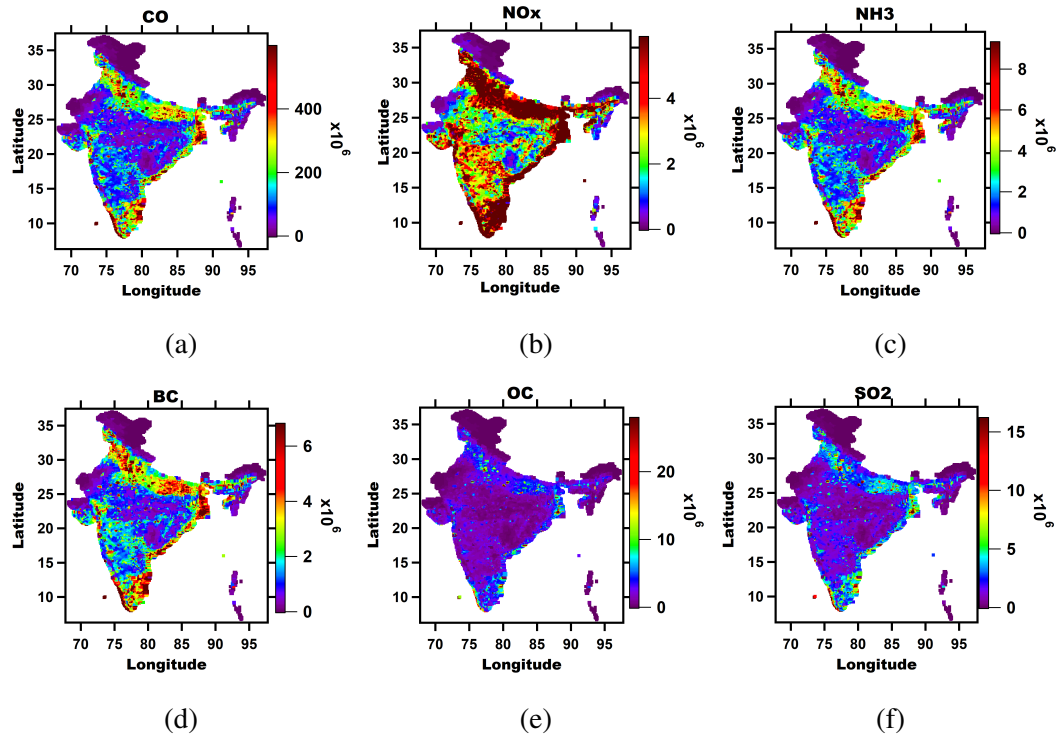


Figure 2.11: The gridded maps of waste burning emission of CO, NO_x, NH₃, BC, OC, SO₂ from the OWBEII. The emissions are in the units of g/year[15].

Chapter 3

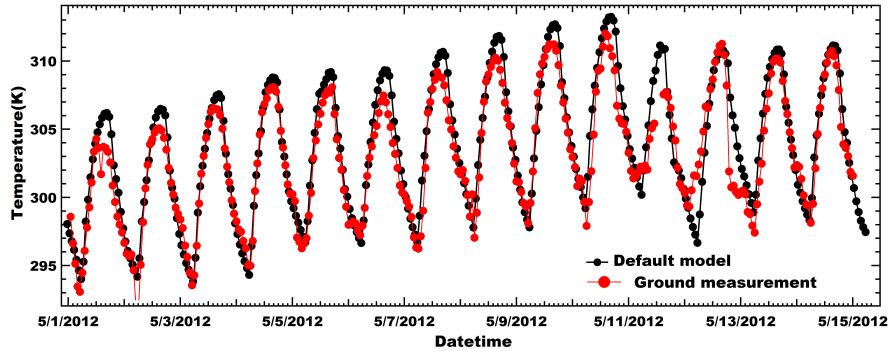
Results and discussions

3.1 Results of the default model simulation

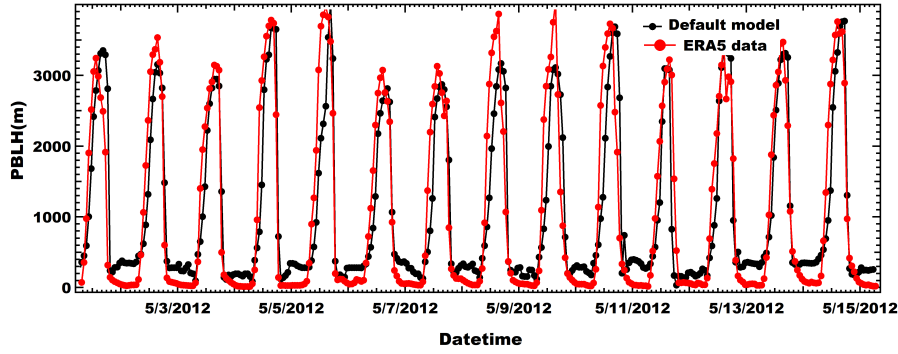
The meteorological parameters are very crucial to the atmospheric transport model. Meteorological fields significantly affect the atmospheric chemistry and transport of chemical species. So we looked at the temperature, planetary boundary layer height, and the solar radiation of the default modelling setup.

As we can see in the Figure3.1, the simulated temperature and the PBLH are in good agreement with the ground measurement and the ERA5 reanalysis data, respectively. PBLH affects the momentum and heat fluxes between the earth surface and atmosphere. It also perturbs the mixing and concentration of the chemical species. The solar radiation simulated by the model agrees with the recorded data, except the peak values show little high readings. Since our model setup can reproduce the meteorological parameters within small errors, we have used this setup for further study without any modifications.

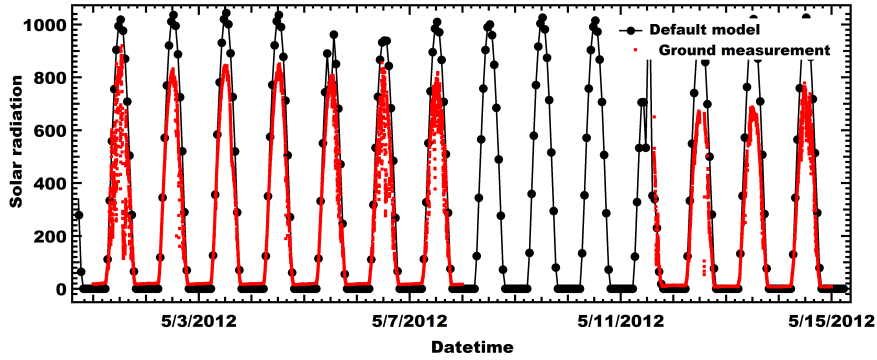
We looked at the time series of a few chemical species to see the accuracy of EDGARv4.3.2 in our modelling domain. In Figure3.2, the simulated CO and NO_x show good agreement with the ground data, while the model significantly underestimates the NMVOCs. The model is unable to capture the high emission events, but it follows the diurnal variability for CO and NO_x nicely.



(a)

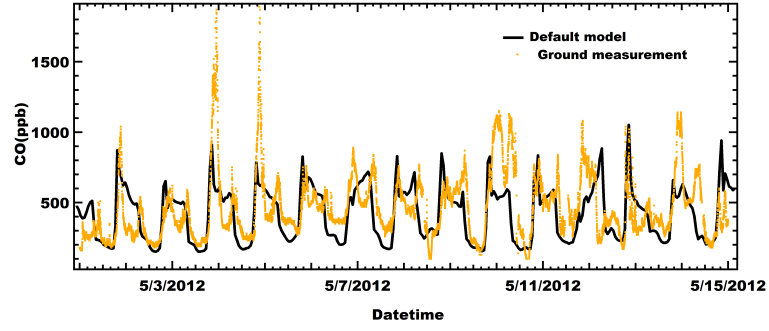


(b)

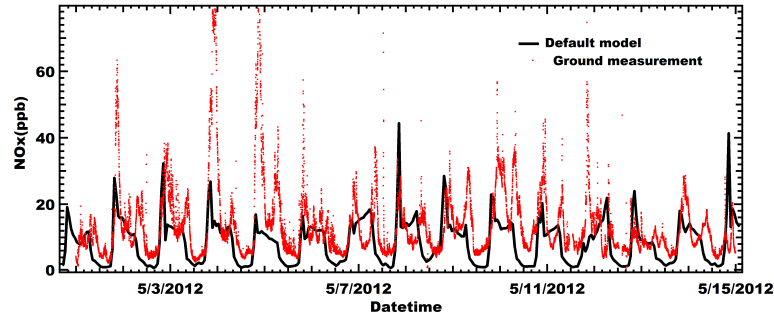


(c)

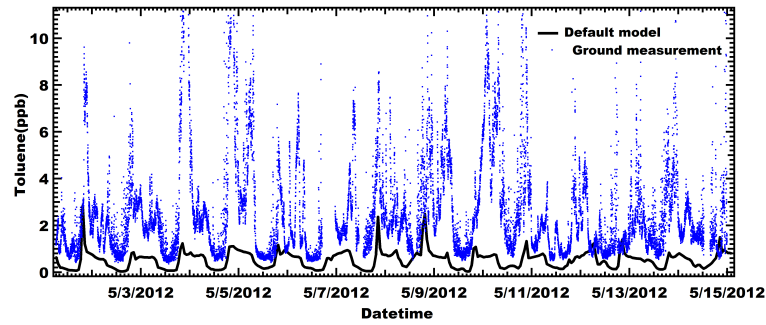
Figure 3.1: The meteorological parameters simulated using the default model extracted over Mohali and compared with ground measurement data. 3.1a shows the time series of temperature, 3.1b shows the time series of PBLH compared with the ERA5 reanalysis product, and 3.1c is the solar radiation time series plot against the ground measurement data.



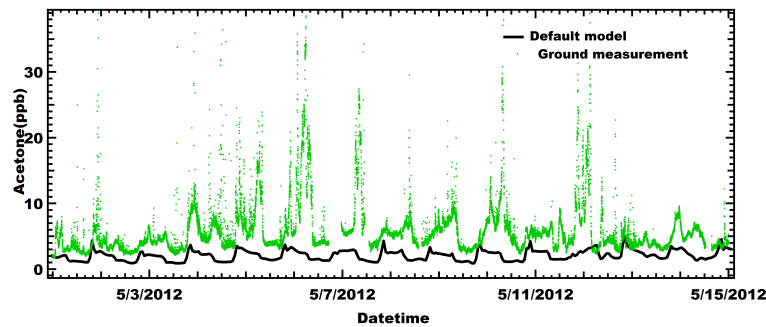
(a)



(b)



(c)



(d)

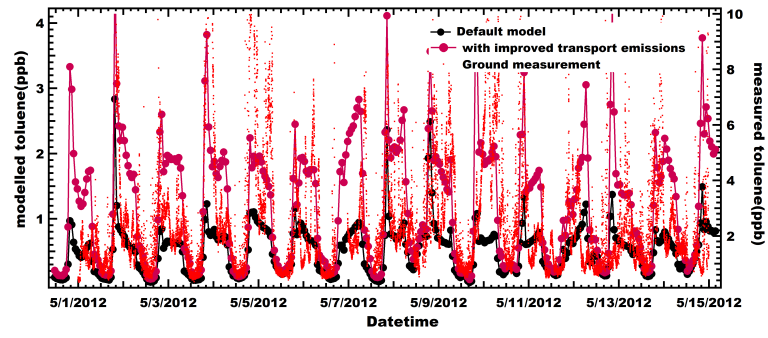
Figure 3.2: Time series of the criteria air pollutants like carbon monoxide(CO) and nitrogen oxides(NO_x) along with the NMVOCs toluene and acetone simulated by the default model. Modelled quantities are plotted along the left axis and ground measurement based quantities are plotted along the right axis.

3.2 Sensitivity of the new road-transport emission inventory(RTEII)

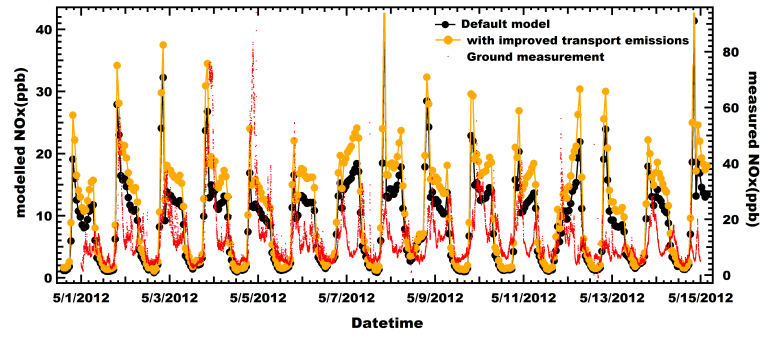
To study the sensitivity of the new road transport emission inventory(RTEII), firstly, we compared the time series of various species, mainly which are among the top 10 highest emitted VOCs and show significant difference from the default model. As shown in Figure 3.3, toluene, NO_x , and acetaldehyde show a significant increase in emissions. Whereas emission of carbon monoxide decrease over Mohali. These differences can be directly attributed to the new road-transport emissions used in the improved model. Even after addition of the road transport inventory the emissions of NMVOCs are quite low in comparison with the ground measurement data.

To understand the spatial differences in the emissions from two scenarios, we looked at the spatial maps of emissions over the modelling domain. The WRF-Chem model was set to dump the output files at an hourly interval. So we had the emission data of each hour for entire simulation period. We first took the average of all hourly emissions at each gridpoint for both the scenarios. Then we subtracted default emissions from the improved emissions and plotted the percentage difference at each lat-lon. Figure 3.4 shows the gridded maps of the top compounds, which have the highest differences in emissions between the two scenarios. The first two columns represent the average emission of each species and the third column represents the percentage difference between the two scenarios at each gridpoint. The emission of acetaldehyde increases by 24% after adding the new road transport sector to the EDGAR. Toluene and NO_x increase by 23% each. Acetone emission is also increased by 13%, while CO emission is decreased by 8%.

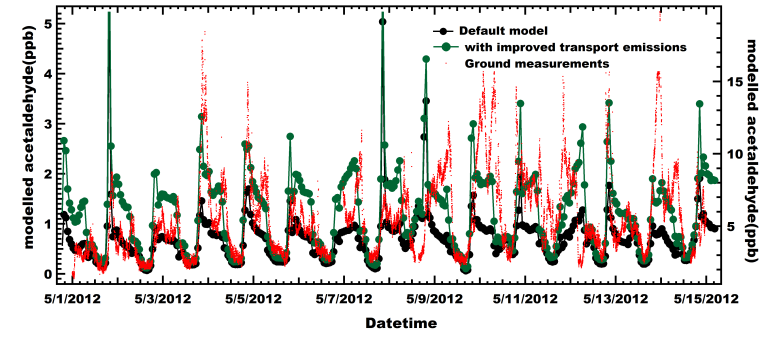
In most pollutants, an extreme increase in emissions is observed over Delhi and its surrounding regions. Delhi is the capital of India and is one of the most crowded cities in India. It is highly affected by road transport emissions. Toluene is the most prevailing compound of the BTEX family known to be emitted by vehicle emissions. An increase of around 100% is observed in the toluene emission over Delhi and around 25-50% over the cities(Chandigarh, Shrinagar) in the north part of the domain. Acetaldehyde also shows a similar trend, an increase of around 100% is observed in Delhi emissions. Acetone also shows a significant increase in the emissions in the lower part of the domain. On the other hand, CO is underestimated by the improved transport model. The most significant decrease



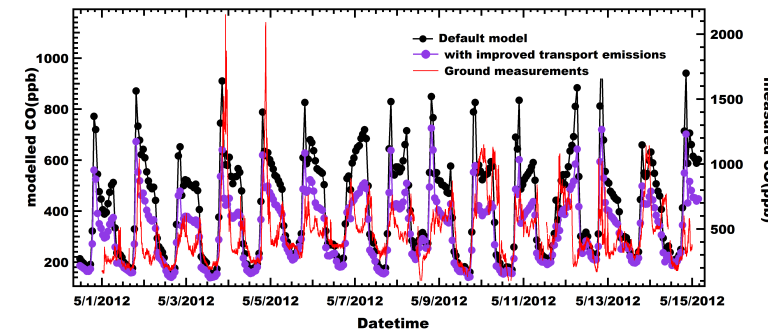
(a)



(b)



(c)



(d)

Figure 3.3: The time series of (a) toluene, (b) NO_x , (c) acetaldehyde, and (d) CO for default and improved road-transport model extracted over Mohali.

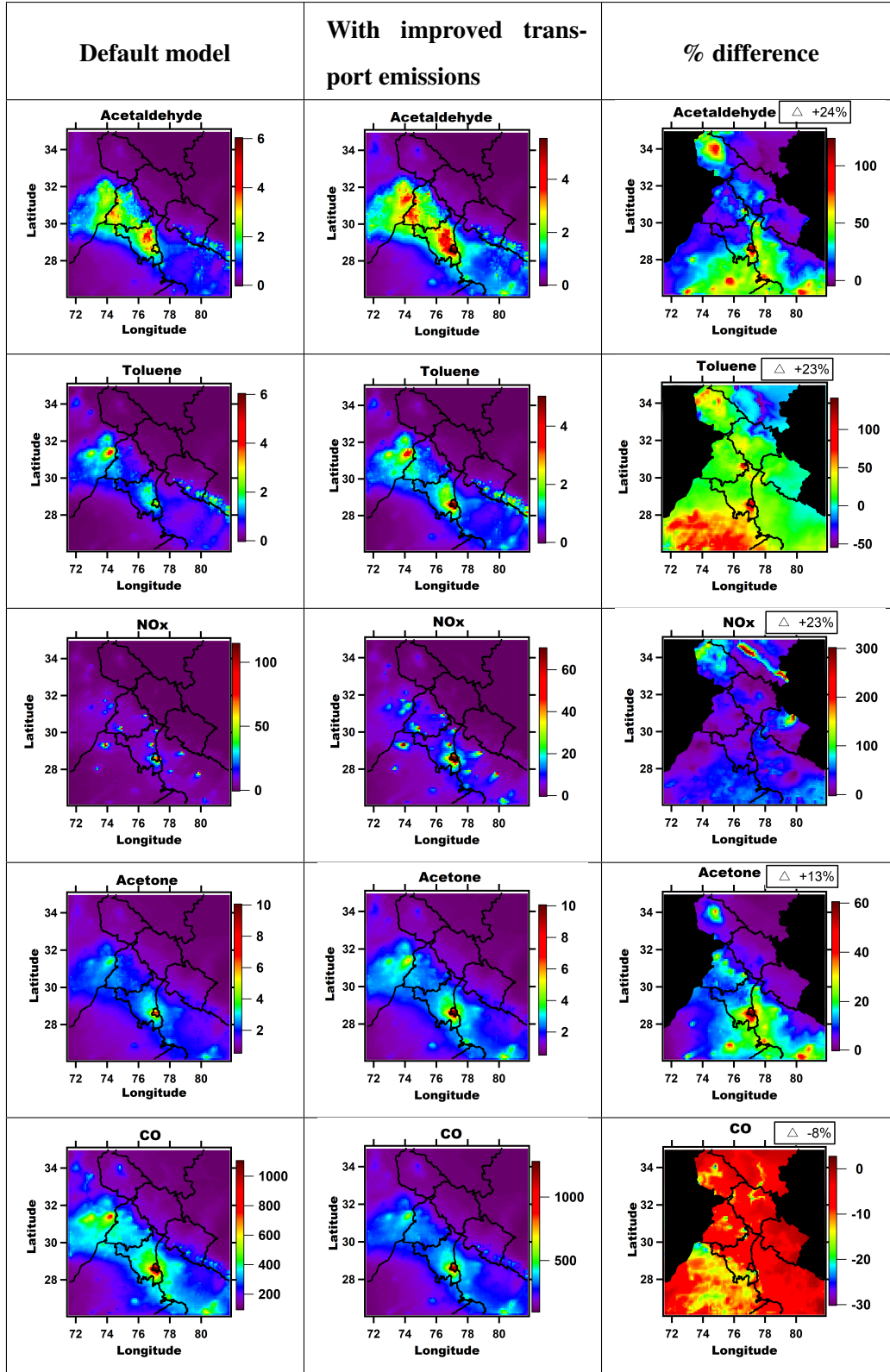


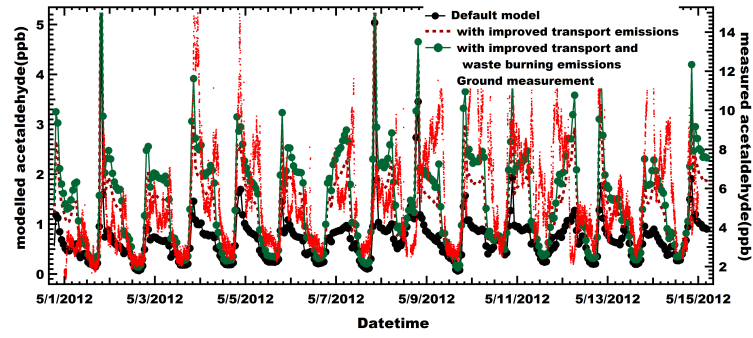
Figure 3.4: The spatial maps of the average emissions of acetaldehyde, toluene, NO_x, acetone, and CO. The emissions of the default model(column 1),after using improved transport emissions(column 2), and the percentage difference between two scenarios(column 3){(improved emission-default emission) \times 100/default emission} at each grid point is shown. The total percentage difference is calculated using average of emissions over complete domain for entire simulation.

is seen in the emissions of Rajasthan.

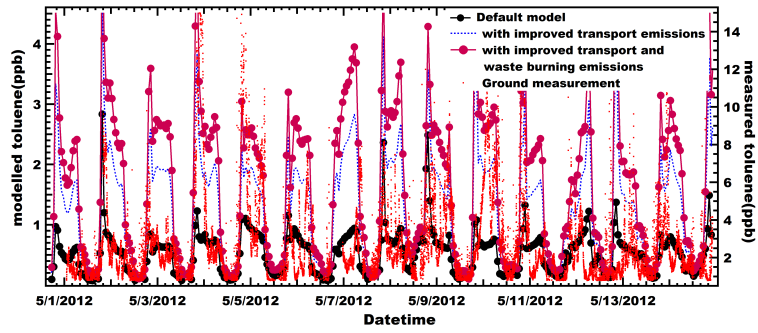
3.3 Results of adding the waste burning sector to EDGARv4.3.2

We added the new open waste burning inventory to the EDGARv4.3.2, which already had the improved road-transport sector. We incorporated this improved EDGAR inventory into the WRF-chem code and ran the third scenario, the improved road-transport and waste burning. Figure 3.5 shows the time series of emissions for VOCs simulated by the improved road transport and waste burning model. 3.5a presents the time series of acetaldehyde compared with default and the improved road-transport model. We observe the higher daytime emission of acetaldehyde coming from the open waste burning. A similar result we have observed for toluene, the open waste burning sector is sensitive to the toluene emission over the Mohali lat-lon. On the other hand, the time series of carbon monoxide is not affected by the addition of the waste burning sector at this particular grid point. The time series of propene shows lower peak values than the default scenario, but the emissions are higher relative to the modified road-transport model. This suggests the increase in propene emission because of the waste burning sector over Mohali. CO and NO_x simulated by the improved model show better agreement with ground based measurements, but NMVOCs still show the underestimation in emissions.

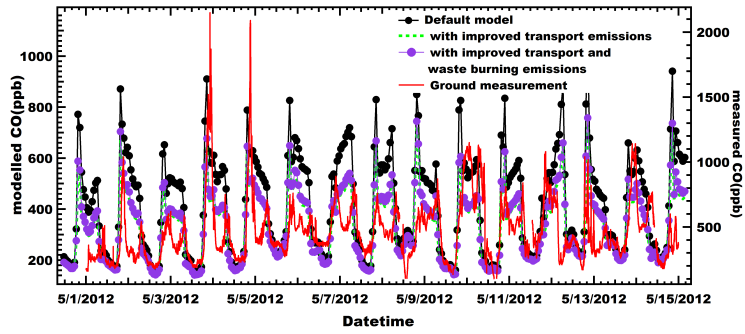
Figure 3.6 shows the gridded maps of average emissions of the selected VOCs for the default and the modified waste burning models. The third column represents the percentage difference between the average emission of both models at each gridpoint. Acetaldehyde emissions simulated with the improved road transport and waste burning sectors is highly overestimated(35%) relative to the EDGARv4.3.2. Toluene also indicates an increment of 30% relative to the default model and an increment of 7% relative to the improved road-transport model. NO_x and acetone have increased by 3% each from the improved road transport scenario. NO_x is increased by 26%, and acetone is increased by 17% when compared to the default scenario. Carbon monoxide emission is underestimated(-6%) relative to the default model setup, but it has increased by 2% relative to the improved road-transport model. This increase in the emission of CO is coming from the new waste burning sector. The spatial increase in the emissions of the species can also be studied. Acetaldehyde and



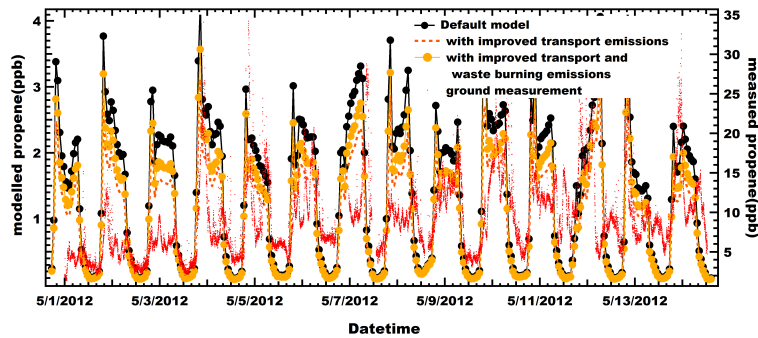
(a)



(b)



(c)



(d)

Figure 3.5: The time series of (a) acetaldehyde, (b) toluene, (c) CO, and (d) propene for default and improved road transport and waste burning model extracted over Mohali. Modelled quantities are plotted along the left axis and ground measurement based quantities are plotted along the right axis.

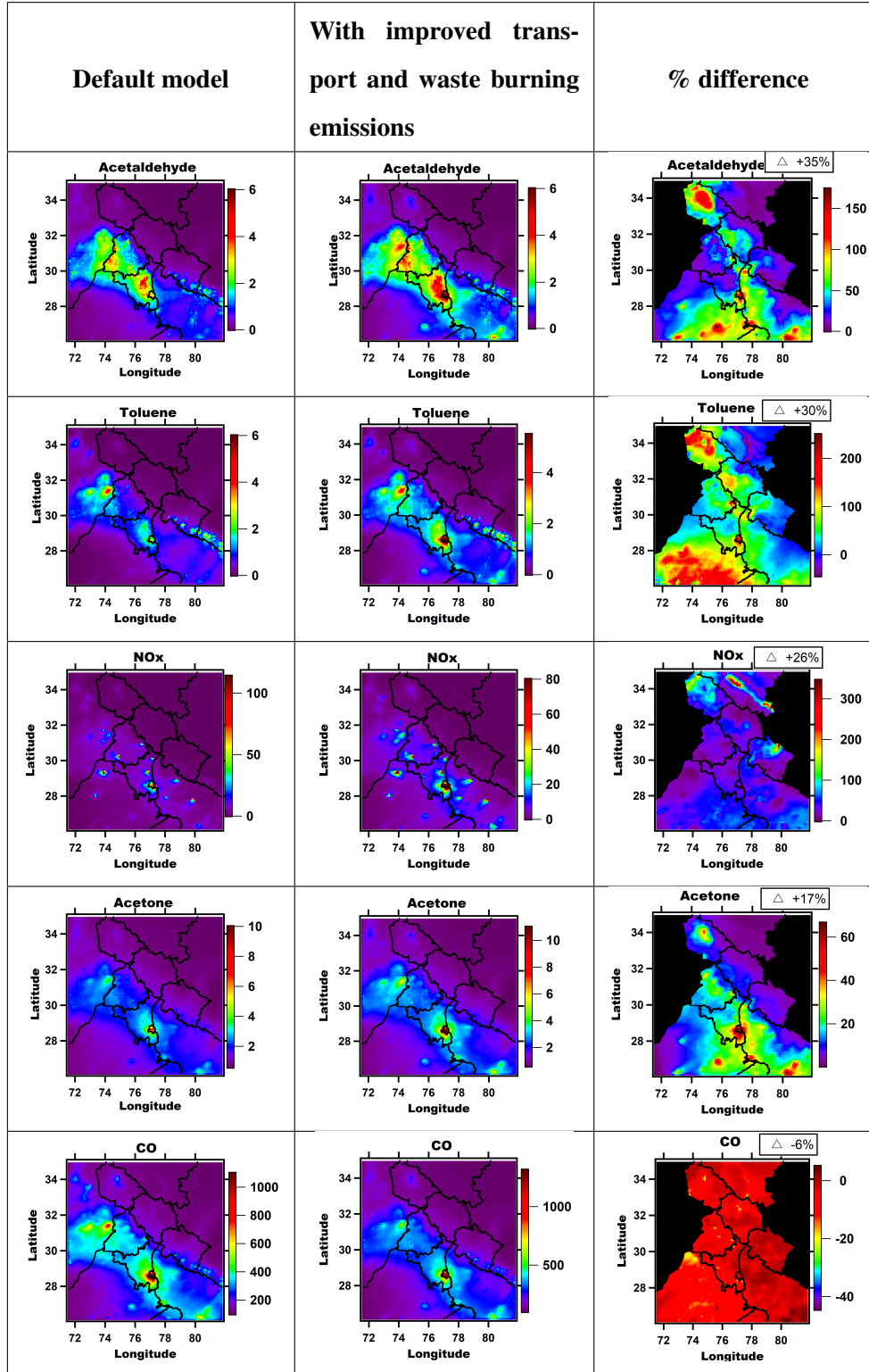
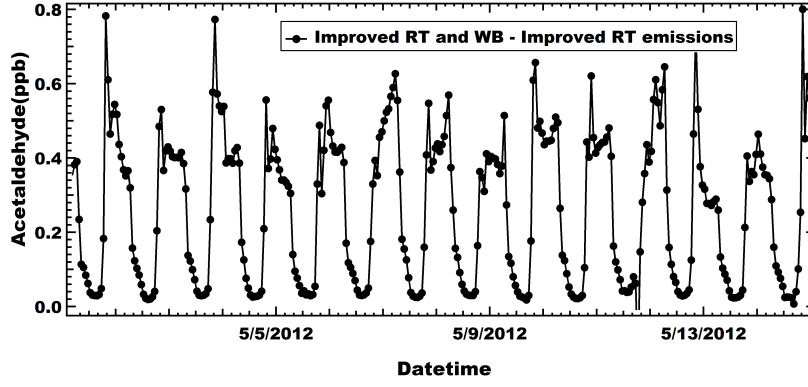
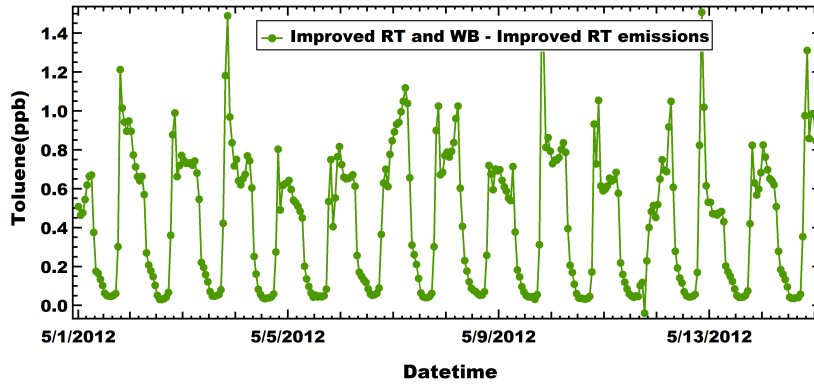


Figure 3.6: The gridded maps of the average emissions of acetaldehyde, toluene, NO_x, acetone, and CO. The emissions of the default model(column 1), the improved road transport and waste burning model(column 2), and the percentage difference between two scenarios(column 3) $\{(\text{improved emission} - \text{default emission}) \times 100 / \text{default emission}\}$ are shown. The total percentage difference is calculated using average of emissions over complete domain for entire simulation.



(a)



(b)

Figure 3.7: The time series of difference between the emissions of two modelling scenarios: with improved road transport and waste burning emissions minus with improved road transport emissions for (a) acetaldehyde and (b) toluene extracted over Mohali.

toluene show significant increase of around 150% and 200%, respectively, over Delhi after addition of the improved waste burning and transport emissions. Emissions of toluene over Himachal Pradesh and Punjab coming from waste burning sector are increased.

Addition of the improved waste burning emissions on the top of road transport emissions further increase the modelled emissions. Figure 3.7 shows the time series of the difference between emissions of these two scenarios over IISER Mohali for acetaldehyde and toluene. We see significant increase of around 0.5 to 0.9 ppb in daytime acetaldehyde. In addition, we see around 0.6 to 1.4 ppb increase in daytime toluene after adding improved waste burning emissions.

Chapter 4

Summary and conclusion

The WRF-Chem model set up was validated for the North-India domain. The WRF-Chem model was run for the first ten days of August 2012 with the revised plant functional types map, ERA5 leaf area index dataset, and vegetation fraction dataset. The simulated meteorological fields were compared with the published study by Mishra *et al.*.

The validated WRF-Chem was applied to look at the air quality changes in criteria air pollutants and VOCs over north India. The sensitivity study of the newly created road transport emission inventory and the open waste burning emission inventory from India was conducted. The EDGARv4.3.2 inventory used in the WRF-chem model set up for the time period of 1 May – 14 May 2012 performed well over the North India. The meteorological parameters for this set up were in good agreement with the ground measurement data collected at the atmospheric facility at IISER Mohali. The road-transport sector of the EDGARv4.3.2 was replaced by the RTEII. The OWBEII was added to the EDGARv4.3.2 as a new waste burning sector. The WRF-Chem model was run for three different scenarios to study the sensitivity of these new emission sectors. The WRF-Chem simulation study found acetaldehyde and toluene to be the top NMVOCs emitted by the road-transport and waste burning sectors which have been highly underestimated by EDGARv4.3.2. The EDGARv4.3.2 inventory underestimates NO_x relative to the RTEII, whereas it overestimates CO. Acetone was found to be underestimated by EDGARv4.3.2 relative to both the inventories.

Appendix A

Important codes for the input files used in WRF-Chem

A.1 Anthropogenic emission input file

```
1 &CONTROL
2 anthro_dir = '/home/abhi/Build_WRF/Emission_inp_Data/Anthro_inp'
3 src_file_prefix = 'EDGAR_HTAP_emi_'
4 src_file_suffix = '_2010.0.1x0.1.nc'
5 src_names = 'CO(28)', 'NOx(30)', 'BIGALK(72)', 'BIGENE(56)', 'C2H4(28)
6             ', 'C2H5OH(46)',
7             'C2H6(30)', 'C3H6(42)', 'C3H8(44)', 'CH2O(30)', 'CH3CHO(44)
8             ', 'CH3COCH3(58)',
9             'CH3OH(32)', 'MEK(72)', 'SO2(64)', 'TOLUENE(92)', 'NH3(17)
10            ',
11            'OC(12)', 'BC(12)'
12 sub_categories = 'emis_tot'
13 emis_map = 'CO->CO', 'NO->NOx', 'BIGALK->BIGALK', 'BIGENE->BIGENE', '
14            C2H4->C2H4', 'C2H5OH->C2H5OH',
15            'C2H6->C2H6', 'C3H6->C3H6', 'C3H8->C3H8', 'CH2O->CH2O', '
16            CH3CHO->CH3CHO',
17            'CH3COCH3->CH3COCH3', 'CH3OH->CH3OH', 'MEK->MEK', 'SO2->SO2
18            ', 'TOLUENE->TOLUENE',
19            'NH3->NH3', 'OC(a)->OC', 'BC(a)->BC'
20 serial_output = .false.
```

```

15  start_output_time = '2012-05-01_00:00:00'
16  data_yrs_offset =2
17 /

```

A.2 Fire emission input file

```

1 &control
2  domains          = 1,
3      fire_directory = '/home/abhi/Build_WRF/Emission_utl/Fire/
      data_files/',
4  fire_filename     = 'GLOBAL_FINNv15_2012_MOZ4_7112014.txt',
5
6  wrf_directory     = '/home/abhi/Build_WRF/Emission_utl/Fire/',
7  start_date        = '2012-04-28',
8  end_date          = '2012-05-15',
9
10     wrf2fire_map = 'co -> CO', 'no -> NO', 'so2 -> SO2', 'bigalk
      -> BIGALK',
11     'bigene -> BIGENE', 'c2h4 -> C2H4', 'c2h5oh -> C2H5OH',
12     'c2h6 -> C2H6', 'c3h8 -> C3H8', 'c3h6 -> C3H6', 'ch2o ->
      CH2O', 'ch3cho -> CH3CHO',
13     'ch3coch3 -> CH3COCH3', 'ch3oh -> CH3OH', 'mek -> MEK', '
      toluene -> TOLUENE',
14     'nh3 -> NH3', 'no2 -> NO2', 'open -> BIGALD', 'c10h16 ->
      C10H16',
15     'ch3cooh -> CH3COOH', 'cres -> CRESOL', 'glyald -> GLYALD
      ', 'mgly -> CH3COCHO',
16     'gly -> CH3COCHO', 'acetol -> HYAC', 'isop -> ISOP', 'macr
      -> MACR', 'mvk -> MVK',
17     'oc -> OC; aerosol ', 'pm10 -> PM10; aerosol ', 'pm25 -> PM25;
      aerosol ',
18     'bc -> BC; aerosol '
19
20 /

```

Bibliography

- (1) Ohara, T.; Akimoto, H.; Kurokawa, J.; Horii, N.; Yamaji, K.; Yan, X.; Hayasaka, T. *Atmospheric Chemistry and Physics* **2007**, 7, 4419–4444.
- (2) Colvile, R. N.; Hutchinson, E. J.; Mindell, J. S.; Warren, R. F. The transport sector as a source of air pollution, 2001.
- (3) Singh, R.; Sharma, C.; Agrawal, M. *Transportation Research Part D: Transport and Environment* **2017**, 52, 64–72.
- (4) MORTH *Annual Report 2011–12*, Ministry of Road Transport and Highways, Government of India, New Delhi, India. Tech. rep.; 2014.
- (5) Pallavi; Sinha, B.; Sinha, V. *Atmospheric Chemistry and Physics* **2019**, 19, DOI: 10.5194/acp-19-15467-2019.
- (6) Huang, G.; Brook, R.; Crippa, M.; Janssens-Maenhout, G.; Schieberle, C.; Dore, C.; Guizzardi, D.; Muntean, M.; Schaaf, E.; Friedrich, R. *Atmospheric Chemistry and Physics Discussions* **2017**, 1–36.
- (7) Hakkim, H.; Kumar, A.; Annadate, S.; Sinha, B.; Sinha, V. *personal communication* **2021**.
- (8) Hoornweg, D.; Bhada-Tata, P. *Urban Development - What a Waste: A Global Review of Solid Waste Management*; tech. rep.; 2012, p 94.
- (9) Wiedinmyer, C.; Yokelson, R. J.; Gullett, B. K. *Environmental Science and Technology* **2014**, 48, 9523–9530.
- (10) Kumar, S.; Smith, S. R.; Fowler, G.; Velis, C.; Kumar, S. J.; Arya, S.; Rena; Kumar, R.; Cheeseman, C. Challenges and opportunities associated with waste management in India, 2017.

- (11) Nagpure, A. S.; Ramaswami, A.; Russell, A. *Environmental Science and Technology* **2015**, *49*, DOI: 10.1021/acs.est.5b03243.
- (12) Ramaswami, A.; Baidwan, N. K.; Nagpure, A. S. *Waste Management and Research* **2016**, *34*, DOI: 10.1177/0734242X16659924.
- (13) CPCB *Consolidated annual review report on implementation of solid wastes management rules, 2016*; tech. rep. 4; 2017.
- (14) Sinha, B. Sharma, G. Sinha, Baerbel; sharma, Gaurav; Jangra, Pallavi; Hakim, Haseeb; Chandra, Boggarapu Praphulla ; Sharma, Ashish Kumar; Sinha, Vinayak (2020), "Gridded emissions of CO, NO_x, SO₂, CO₂, NH₃, HCl, CH₄, PM_{2.5}, PM₁₀, BC and NMVOCs emissions from open municipal wa, 2020.
- (15) Sharma, G.; Sinha, B.; Pallavi; Hakkim, H.; Chandra, B. P.; Kumar, A.; Sinha, V. *Environmental Science and Technology* **2019**, *53*, DOI: 10.1021/acs.est.8b07076.
- (16) Li, M. et al. *Atmospheric Chemistry and Physics* **2017**, *17*, DOI: 10.5194/acp-17-935-2017.
- (17) Greenstone, M.; Nilekani, J.; Pande, R.; Ryan, N.; Sudarshan, A.; Sugathan, A. *Economic and Political Weekly* **2015**, *50*.
- (18) NCEP NCEP FNL Operational Model Global Tropospheric Analyses, continuing from July 1999. Research Data Archive at the National Center for Atmospheric Research, Computational and Information Systems Laboratory. Accessed 10/01/20, Boulder CO, 2000.
- (19) Guenther, A.; Karl, T.; Harley, P.; Wiedinmyer, C.; Palmer, P. I.; Geron, C. *Atmospheric Chemistry and Physics* **2006**, *6*, DOI: 10.5194/acp-6-3181-2006.
- (20) Guenther, A. *Journal of Geophysical Research* **1995**, DOI: 10.1029/94JD02950.
- (21) Guenther, A. B.; Jiang, X.; Heald, C. L.; Sakulyanontvittaya, T.; Duhl, T.; Emmons, L. K.; Wang, X. *Geoscientific Model Development* **2012**, DOI: 10.5194/gmd-5-1471-2012.
- (22) Chandra, B. P.; Sinha, V. *Environment International* **2016**, *88*, 187–197.

- (23) Wiedinmyer, C.; Akagi, S. K.; Yokelson, R. J.; Emmons, L. K.; Al-Saadi, J. A.; Orlando, J. J.; Soja, A. J. *Geoscientific Model Development* **2011**, *4*, DOI: 10 . 5194/gmd-4-625-2011.
- (24) Mishra, A. K.; Sinha, B.; Kumar, R.; Barth, M.; Hakkim, H.; Kumar, V.; Kumar, A.; Datta, S.; Guenther, A.; Sinha, V. *Science of the Total Environment* **2021**, DOI: 10.1016/j.scitotenv.2020.141728.
- (25) FRIEDL, M. A.; STRAHLER, A. H.; HODGES, J. ISLSCP II MODIS (Collection 4) IGBP Land Cover, 2000-2001, 2010.
- (26) Chen, F.; Dudhia, J. *Monthly Weather Review* **2001**, *129*, DOI: 10 . 1175/1520-0493 (2001) 129<0587:CAALSH>2 . 0 . CO; 2.
- (27) Janssens-Maenhout, G.; Dentener, F.; Aardenne, J. V.; Monni, S.; Pagliari, V.; Orlandini, L.; Klimont, Z.; Kurokawa, J.-i.; Akimoto, H.; Ohara, T.; Wankmüller, R.; Battye, B.; Grano, D.; Zuber, A.; Keating, T., *EDGAR-HTAP: a harmonized gridded air pollution emission dataset based on national inventories*, 2012.
- (28) Hong, S. Y.; Noh, Y.; Dudhia, J. *Monthly Weather Review* **2006**, *134*, DOI: 10 . 1175/MWR3199 . 1.
- (29) Emmons, L. K. et al. *Geoscientific Model Development* **2010**, *3*, DOI: 10 . 5194/gmd-3-43-2010.
- (30) Muñoz Sabater, J. ERA5-Land monthly averaged data from 1981 to present. Copernicus Climate Change Service (C3S) Climate Data Store (CDS). (Accessed on 04-04-2021), 10.24381/cds.68d2bb3, 2019.
- (31) MNGP *National Fuel consumption statistics report 2015-16. Rep., Ministry of 750 Petroleum and Natural Gas, Government of India, New Delhi. Available at: 751 <http://petroleum.nic.in/sites/default/files/pngstat1516.pdf>; tech. rep.; 2016.*